

## Mechanochemical synthesis of Pt/TiO<sub>2</sub> for enhanced stability in dehydrogenation of methycyclohexane

### Supporting Information

Krista Kuutti,<sup>a</sup> Manoj Ghosalya,<sup>b</sup> Paavo Porri,<sup>a</sup> Jacopo De Bellis,<sup>c,1</sup> Päivi Jokimies,<sup>a</sup> Harishchandra Singh,<sup>b</sup> Shubo Wang,<sup>b</sup> Graham King,<sup>d</sup> Javier Fernández-Catalá,<sup>b,e</sup> Ferdi Schüth,<sup>c</sup> Kaisu Ainassaari,<sup>f</sup> Mika Huuhtanen,<sup>f</sup> Marko Huttula,<sup>b</sup> Samuli Urpelainen,<sup>b\*</sup> Sari Rautiainen<sup>a\*</sup>

<sup>a</sup> VTT Technical Research Centre of Finland Ltd, Espoo FI-02044, Finland

<sup>b</sup> Nano and Molecular Systems Research Unit, University of Oulu, 90014 Oulu, Finland

<sup>c</sup> Department of Heterogeneous Catalysis, Max-Planck-Institut für Kohlenforschung, Kaiser-Wilhelm-Platz 1, 45470 Mülheim an der Ruhr, Germany

<sup>d</sup> Canadian Light Source, 44 Innovation Boulevard, Saskatoon, Saskatchewan, S7N 2V3 Canada

<sup>e</sup> Materials Institute and Inorganic Chemistry Department, University of Alicante, Ap. 99, Alicante E-03080, Spain

<sup>f</sup> Environmental and Chemical Engineering Research Unit, University of Oulu, 90014 Oulu, Finland

\* Corresponding authors: sari.rautiainen@vtt.fi, samuli.urpelainen@oulu.fi

1.	General considerations .....	2
1.1.	Reactor set-up .....	2
1.2.	GC analysis .....	2
2.	Reaction optimisation and analysis .....	3
2.1.	Experimental design analysis of MCH dehydrogenation .....	3
2.2.	MCH dehydrogenation side products analysis.....	6
2.3.	Catalyst performance comparison.....	8
3.	Catalyst characterisation .....	8
3.1.	PDF profiles .....	8
3.2.	Particle size analysis of TiO <sub>2</sub> particles.....	9
3.3.	EDS .....	10
3.4.	Particle size analysis of spent catalysts.....	11
3.5.	XPS .....	13
3.6.	In situ APXPS .....	14
3.7.	CO chemisorption .....	15
3.8.	NH <sub>3</sub> temperature programmed desorption .....	16
3.9.	Catalyst comparison to literature .....	17
4.	References.....	17

## 1. General considerations

### 1.1. Reactor set-up

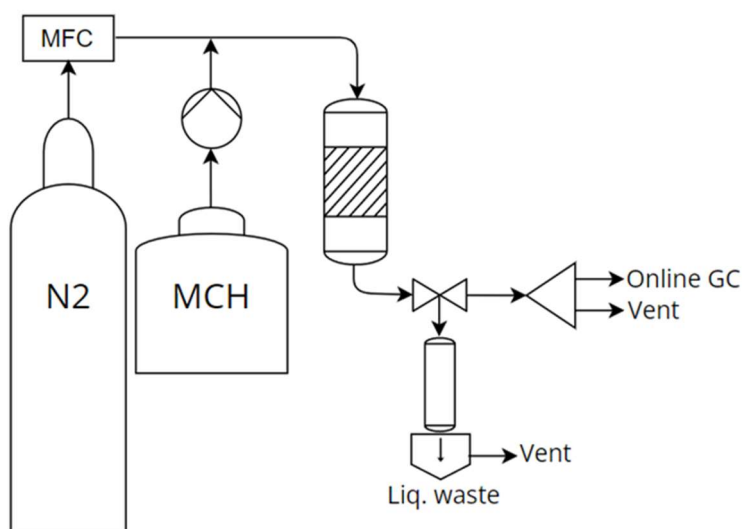


Figure S1. Methylcyclohexane dehydrogenation set-up. MFC stands for mass flow controller.

### 1.2. GC analysis

The Agilent 6890 gas chromatograph was equipped with a magnetic valve system, that passed the gaseous sample first to a precolumn, and after to a capillary column followed by TCD and FID analysis, respectively. The packed precolumn (SS GEN CONFIG) was provided by Restek, and it was packed with Carboxen-1000 molecular sieves. The mesh size was 60/80, length 2.5 m, inner diameter 2.1 mm and outer diameter 1/8 in. The capillary column (DB-1) was provided by Agilent. The column length was 50 m, and inner diameter 0.32 mm. The stationary phase was dimethylpolysiloxane with film thickness of 0.52  $\mu\text{m}$ .

The GC method proceeded as follows. The sample injection volume was 1.00 ml, split ratio 50:1 argon to sample, total flow 99.4 ml/min and temperature 200 °C. Initial oven temperature was 60 °C with 2 min hold time followed by 10 °C/min heating ramp to 115 °C without hold time.

The FID was calibrated by sampling three solutions with known concentrations of MCH and toluene: 75 mol% MCH/25 mol% toluene, 50 mol% MCH/50 mol% toluene, 25 mol% MCH/75 mol% toluene. The solutions were fed through the dehydrogenation set-up without catalyst, but otherwise in the dehydrogenation reaction conditions: N<sub>2</sub> feed rate 50 ml/min, reactor temperature 345 °C and atmospheric pressure. Correction factor for the FID response was then calculated. As expected, there was no difference between MCH and toluene responses, as the FID response should be proportional to the carbon number of a pure hydrocarbon [1]. Furthermore, cyclohexene and benzene were sampled to the GC with a in-house prepared calibration solution containing known weight fractions (~10%) of each constituent, namely cyclohexene, benzene, methylcyclohexane and toluene. This allowed to confirm the assumption of the correction factor for FID response to be 1, and to acquire the retention times for side product analysis. Methane was calibrated with a calibration gas mixture provided by Linde.

The TCD was calibrated by sampling three different volume percentages of nitrogen and hydrogen through the dehydrogenation reactor set-up: 80 vol% N<sub>2</sub>/20 vol% H<sub>2</sub>, 61.5 vol% N<sub>2</sub>/38.5 vol% H<sub>2</sub>, 50 vol% N<sub>2</sub>/50 vol% H<sub>2</sub>. Higher volume percentage of hydrogen than 50% was not sampled, because the dehydrogenation set-up was designed so that such high concentration should not occur, for the TCD response of H<sub>2</sub> was much higher than that of N<sub>2</sub>. The correction factor for H<sub>2</sub> response was 13.6 when that of N<sub>2</sub> was 1.

## 2. Reaction optimisation and analysis

### 2.1. Experimental design analysis of MCH dehydrogenation

The dehydrogenation of MCH was carried out in gas-phase in a continuous flow reactor at atmospheric pressure. Before experimenting with the catalysts, we wanted to have an understanding on the effect of the reaction parameters on the dehydrogenation, and a simple experimental design matrix was used to find the optimal conditions over IWI Pt/TiO<sub>2</sub>. Detailed process description is provided in the main article. MCH conversion in different reactor temperatures and MCH feed rates is plotted versus time on stream in Figure S2. Numeric analysis of the conversion results is presented in Table S1.

The results were fitted using MODDE software version 13.0.2 using partial least squares regression (PLS). A good fit was obtained for MCH conversion ( $R^2=0,90$ ,  $F=9$ ,  $p=0,103$ ), H<sub>2</sub> productivity ( $R^2=0,97$ ,  $F=35$ ,  $p=0,027$ ) and deactivation ( $R^2=0,90$ ,  $F=9$ ,  $p=0,100$ ). The coefficients are shown in Figure S3, and the response surfaces in Figure S4.

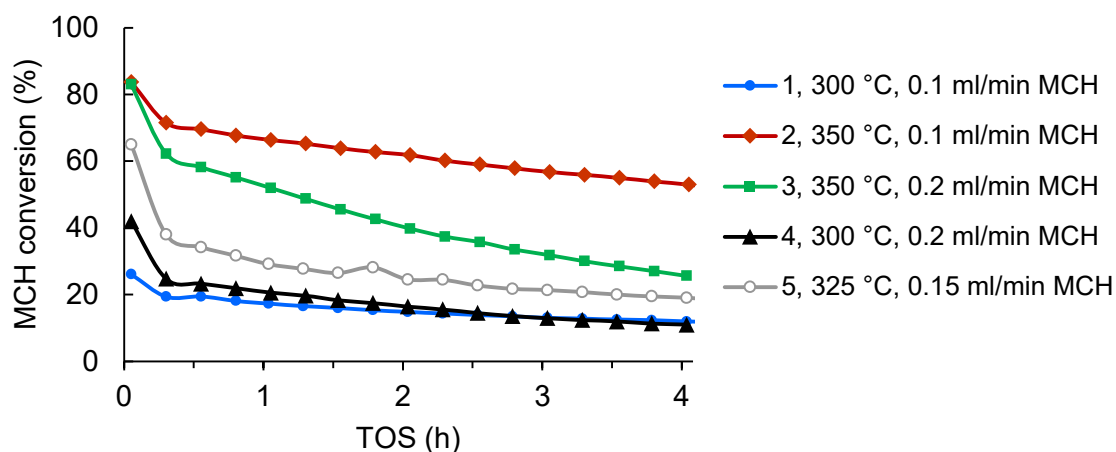


Figure S2. MCH conversion versus time on stream in DOE analysis experiments using IWI Pt/TiO<sub>2</sub>.

Table S1. Results and parameters of the DOE analysis experiments.

Entry	Temperature (°C)	MCH feed rate (ml/min)	Conversion (%) <sup>a</sup>	TOF (mol <sub>H2</sub> /(h*mol <sub>Pt</sub> )) <sup>a</sup>	Deactivation (-Δmol%/h) <sup>b</sup>
1	300	0.1	11.1	1889	1.7
2	350	0.1	53.0	8541	2.9
3	350	0.2	25.7	8136	5.2
4	300	0.2	11.0	3474	4.3
5	325	0.15	19.1	4529	6.8

<sup>a</sup> At 4 hours on stream.

<sup>b</sup> MCH conversion at 18 min minus MCH conversion at 4 h TOS, divided by 3.7 h.

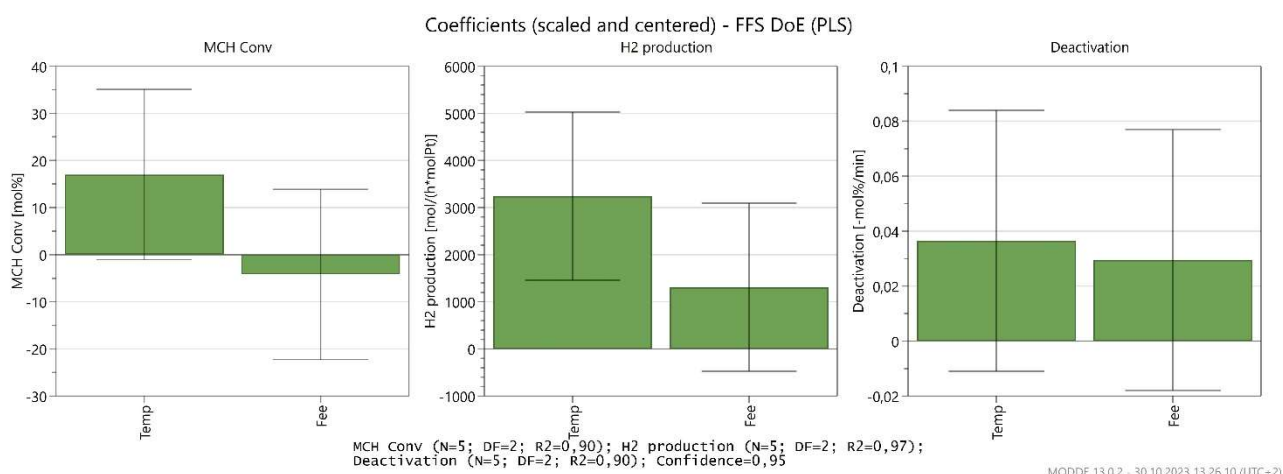


Figure S3. Effect of the studied parameters on the responses. Higher response coefficient corresponds to stronger effect of the respective process parameter on the response in question.

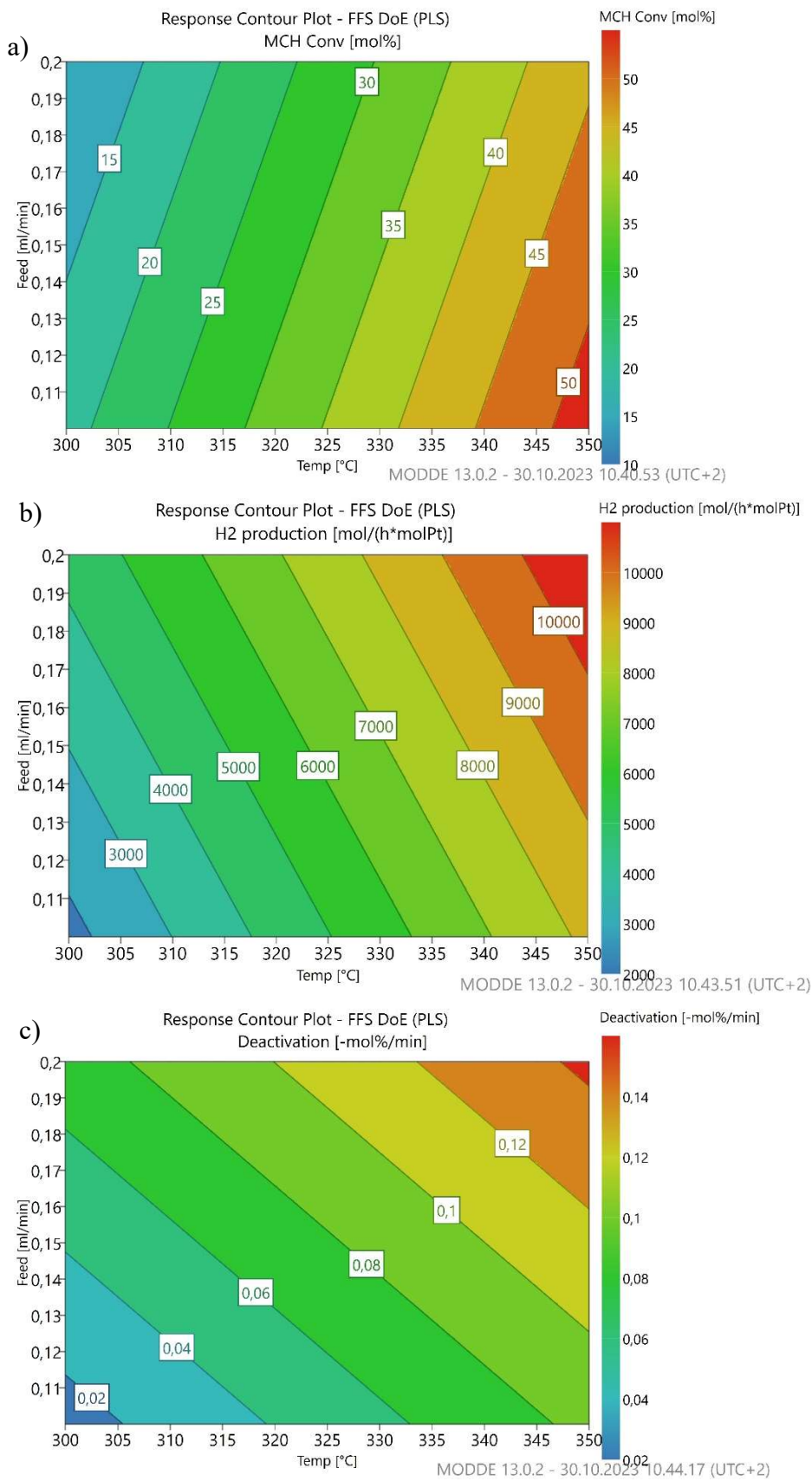


Figure S4. Response surfaces for the DoE analysis of a) MCH conversion, b) TOF and c) deactivation.

## 2.2. MCH dehydrogenation side products analysis

All MCH dehydrogenation experiments had less than 0.5% selectivity to hydrocarbon side products. An exception to this is experiment IWI Pt/TiO<sub>2</sub> 365 °C (Figure S5, datapoint at 7 h TOS), where the side product selectivity is as high as 1.2% at the last datapoint presented. This is caused by the catalyst fully deactivating during the experiment soon after this datapoint. The other experiments had active catalysts throughout the time on stream.

The hydrocarbon side product selectivity plotted in Figure S5 is calculated as a sum of the selectivities of all HC side products detected. These included cyclohexane and benzene, which had their FID-GC retention times confirmed by a calibration solution. However, there were four unidentified products with their retention times close to those of MCH (6.1 min) and toluene (6.7 min). Based on their retention times (6.2, 6.3, 6.5 and 6.8 min), majority of these were suspected to be different isomers of methylcyclohexene. An example FID-chromatogram of experiment IWI 365 °C at 4 h TOS is provided in Figure S6 to illustrate the peak retention. The distribution of the side products to cyclohexane, benzene and the above-described unidentified hydrocarbons is presented in Figure S7. Low levels of CO and CO<sub>2</sub> may form in LOHC hydrogenation/dehydrogenation if the LOHC feed or catalyst contains water or oxygenates [2]. It is plausible that ppm levels of CO and possibly also CO<sub>2</sub> were produced in our system, as the MCH used for the experiments was not specially dried prior to the experiments. However, we could not detect these low ppm levels if they existed, as our online TCD-GC set-up was not sensitive enough for lower than ~1000 ppm level detection of CO and CO<sub>2</sub>.

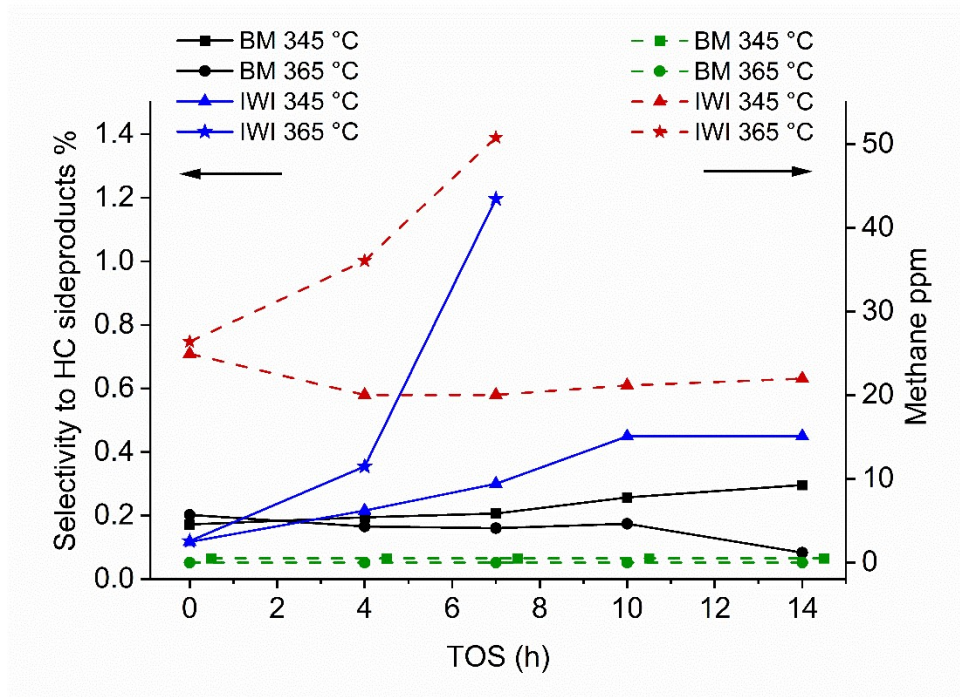


Figure S5. MCH dehydrogenation hydrocarbon side product selectivity and methane production vs. time on stream.

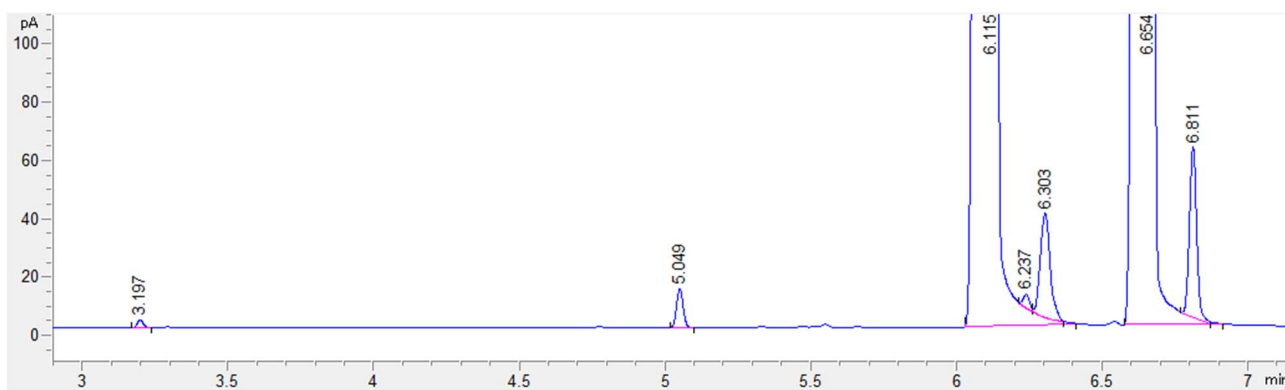


Figure S6. An example FID-chromatogram of experiment IWI 365 °C at 4 h TOS. From left to right (min): 3.197 methane, 5.049 cyclohexane, 6.115 MCH, 6.237 not confirmed, 6.303 not confirmed, 6.654 toluene, 6.811 not confirmed. The MCH and toluene peaks are cropped due to high Y-axis magnification.

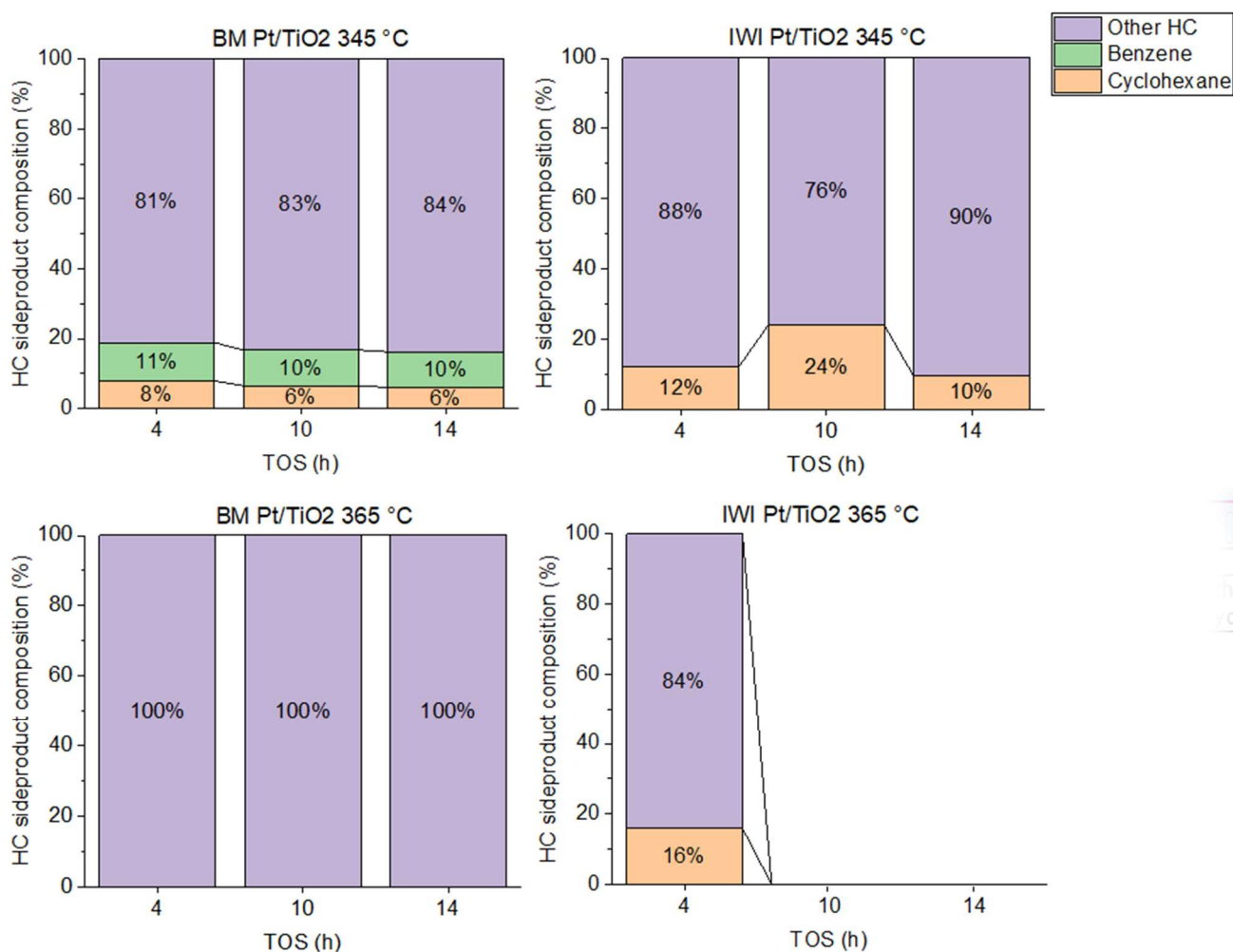


Figure S7. MCH dehydrogenation hydrocarbon side products distribution.

### 2.3. Catalyst performance comparison

Table S2. Catalyst performance in MCH dehydrogenation experiments (atmospheric pressure, liquid MCH feed rate 0.1 ml/min co-fed with 50 ml/min N<sub>2</sub>, 0.2 g catalyst).

Entry	Catalyst	Temp. (°C)	Conversion (%) <sup>a</sup>		TOF (mol <sub>H2</sub> /(h* <sub>molPt</sub> )) <sup>a</sup>		Deactivation (-Δmol%/h) <sup>b</sup>
			TOS 10 min	TOS 15 h	TOS 10 min	TOS 15 h	
1	BM Pt/TiO <sub>2</sub>	345	53	39	7900	5800	1.1
2	IWI Pt/TiO <sub>2</sub>	345	70	44	11700	7300	1.5
3	BM Pt/TiO <sub>2</sub>	365	52	53	7800	8000	0.2
4	IWI Pt/TiO <sub>2</sub>	365	82	0	13600	0	8.8
5 <sup>c</sup>	BM Pt/TiO <sub>2</sub>	345	47	44	7000	7600	0.4

<sup>a</sup> At 15 hours on stream.

<sup>b</sup> Calculated from linear fitting of MCH conversion (mol%) vs. TOS (h) plots.

<sup>c</sup> H<sub>2</sub> co-fed 5 ml/min.

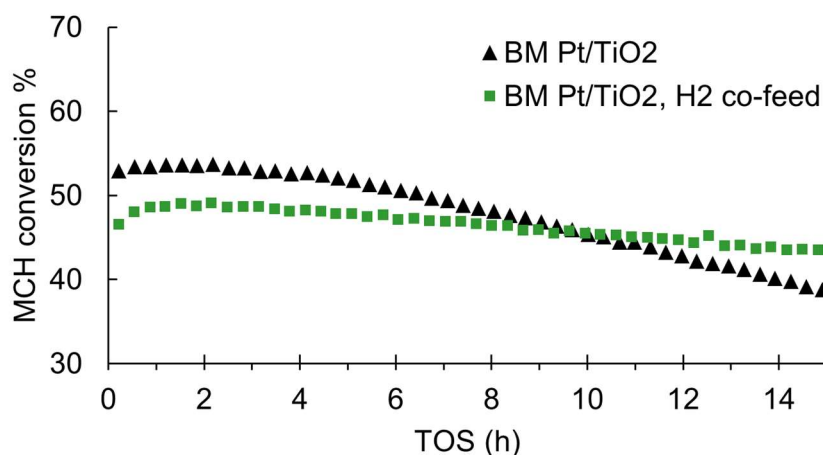


Figure S8. MCH dehydrogenation experiment over BM Pt/TiO<sub>2</sub> catalyst with and without additional hydrogen feed (5 ml/min). Atmospheric pressure, 345 °C temperature, liquid MCH feed rate 0.1 ml/min co-fed with 50 ml/min N<sub>2</sub>, 0.2 g catalyst.

## 3. Catalyst characterisation

### 3.1. PDF profiles

PDF profiles in Figure S9 show structural order in all samples. In general, peaks below 1.8 Å are ripples that do not represent any real structural features. The first peak at 1.95 Å for mainly anatase TiO<sub>2</sub> by wet impregnation and 1.96 Å for rutile TiO<sub>2</sub> by ball milling is ascribed to the average of the first nearest Ti-O correlations (corner and edge sharing local environments) in [TiO<sub>6</sub>] octahedra [3]. Other two weaker peaks around 2.44 and 2.69 Å correlate with O-O pairs with corner- and edge-sharing local environments. These values are similar to the ones in single crystalline rutile and anatase structures, suggesting a strong crystallinity and well-ordered local bonding environments of atoms. Nevertheless, the incorporation of Pt, qualitatively, is likely to induce short-order distortion

of the  $[\text{TiO}_6]$  octahedral structural unit, concerning the weak shoulder humps next to the intense Ti-O correlation peak.

Significant differences in local ordering in the 3–5 Å interval also clearly corroborate the different structured  $\text{TiO}_2$ , consistent with the Bragg diffraction features depicted in Figure 4. Shortening of the nearest Ti-Ti bonding distance, 3.00 vs 2.91 Å in wet impregnated and ball milled samples, and subsequent Ti-Ti,O bonds, 3.78 vs 3.54 Å, is associated with the connectivity of  $[\text{TiO}_6]$  structural unit in rutile and anatase. Such features are expected due to the more compact local atomic packing in rutile than in anatase [4, 5]. Peaks above 5 Å are due to the superposition of multiple atomic pairs, thus are not straightforward to assign.

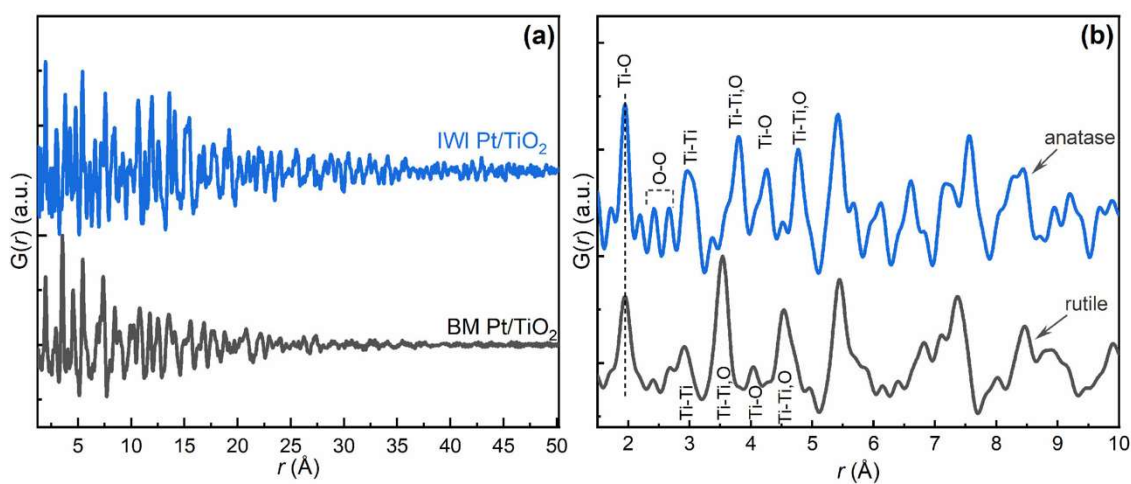


Figure S9. Atomic pair distribution function  $G(r)$  in the  $r$  (interatomic distance) range: (a) 1 to 50 Å, (b) 1-10 Å of the catalyst samples.

### 3.2. Particle size analysis of $\text{TiO}_2$ particles

The mean particle size of the catalyst support particles was deduced from 50 to 70 titania particles discerned in HR-TEM images. The observed particle size of titanium dioxide ( $\text{TiO}_2$ ) exhibited non-uniformity in both examined samples, spanning a range from a few to 70 nm. Notably, the predominant size distribution of titania particles in all samples is concentrated within the range of 10 to 20 nm in good agreement with the XRD findings.

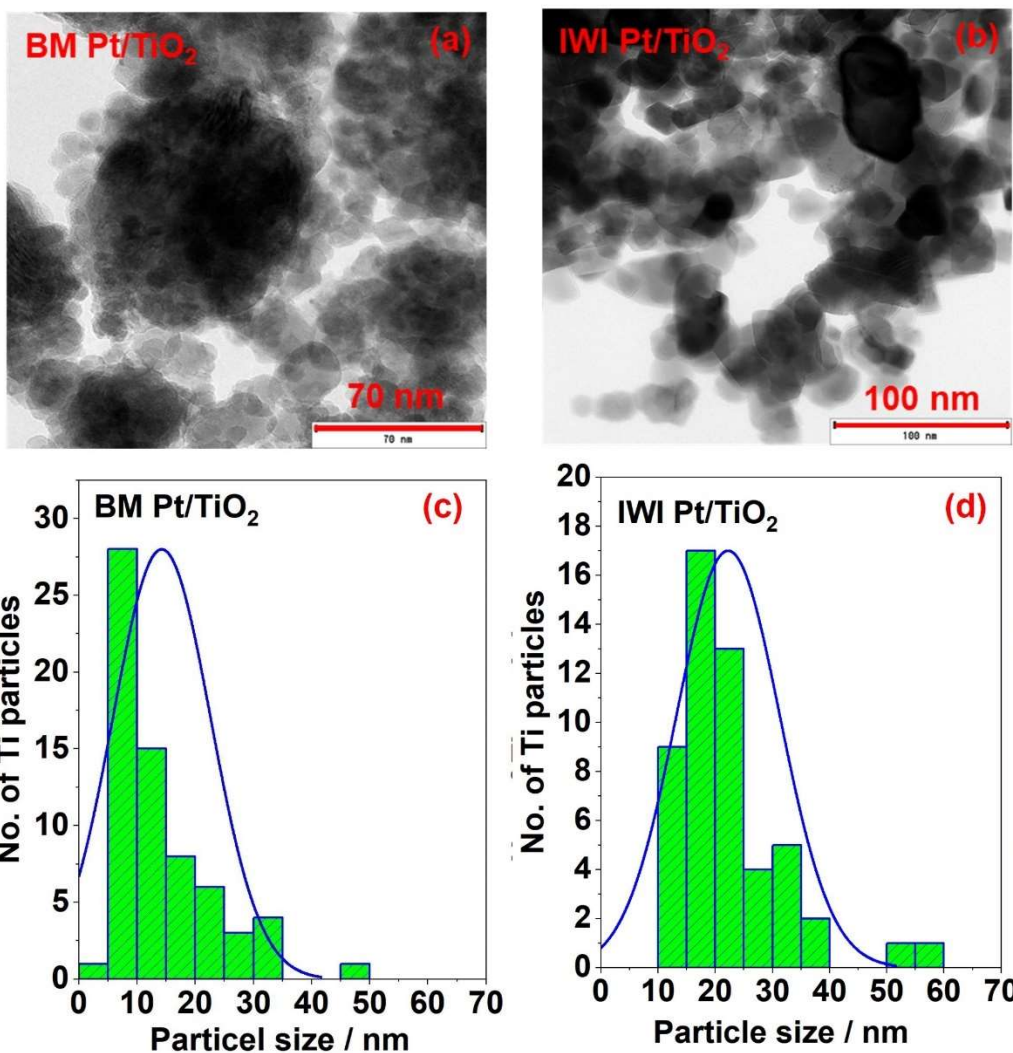


Figure S10. HR-TEM images in panels (a-b) and TiO<sub>2</sub> particles size distribution in panels (c-d). (a, c) BM Pt/TiO<sub>2</sub>, (b, d) IWI Pt/TiO<sub>2</sub>.

### 3.3. EDS

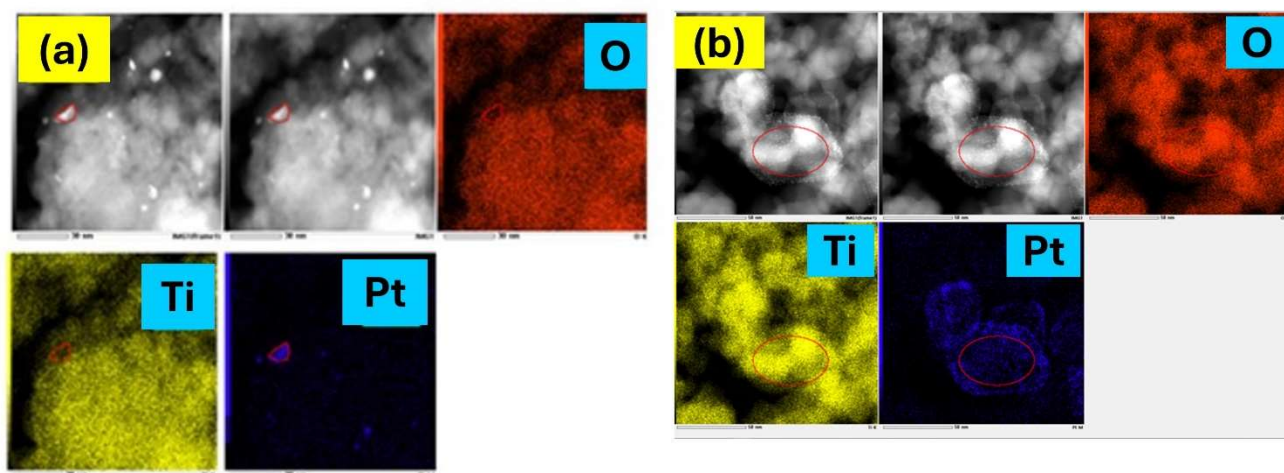


Figure S11. EDS map of (a) BM Pt/TiO<sub>2</sub> (b) IWI Pt/TiO<sub>2</sub>.

### 3.4. Particle size analysis of spent catalysts

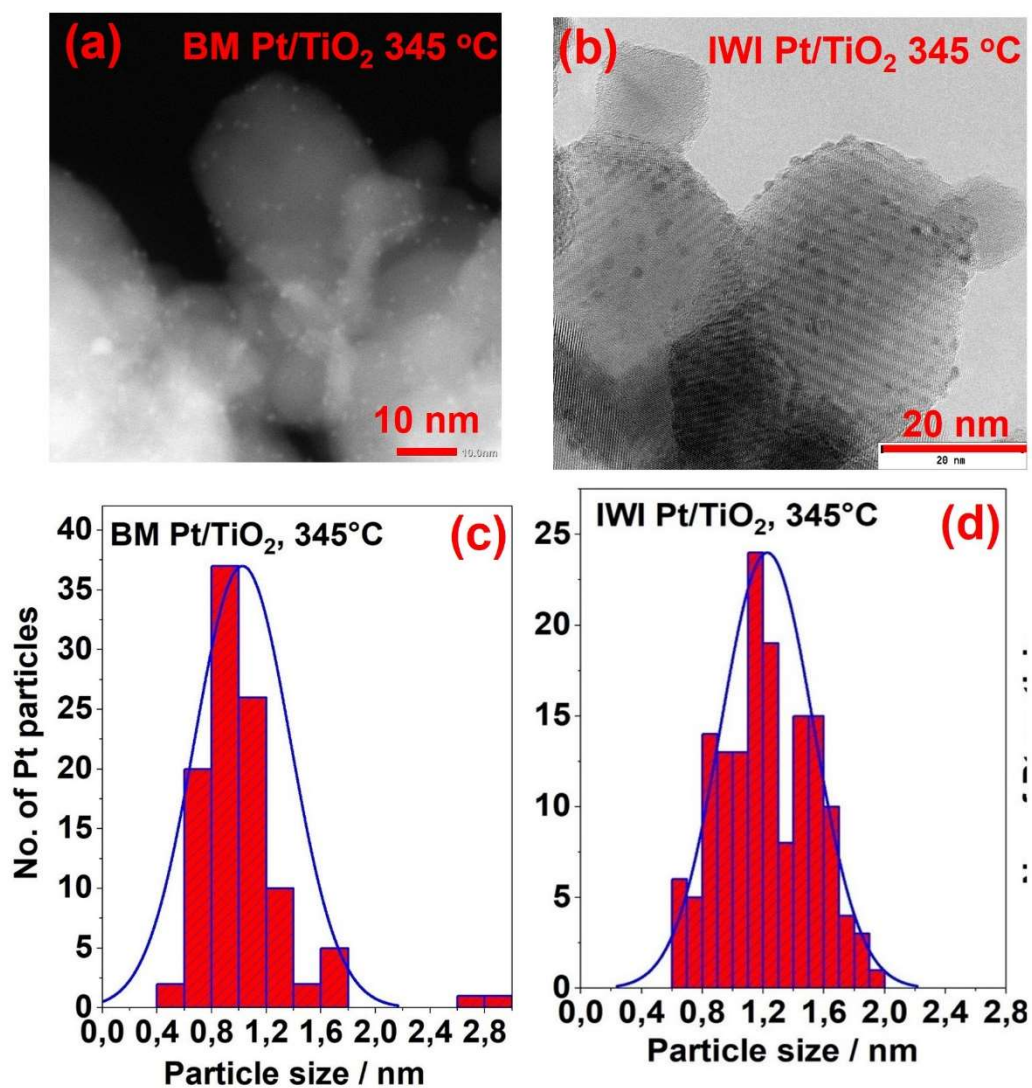


Figure S12. HAADF-STEM images and Pt particle size distributions of the spent catalyst used in MCH dehydrogenation at 345 °C. In panels (a, c) BM Pt/TiO<sub>2</sub> and panels (b, d) IWI Pt/TiO<sub>2</sub>.

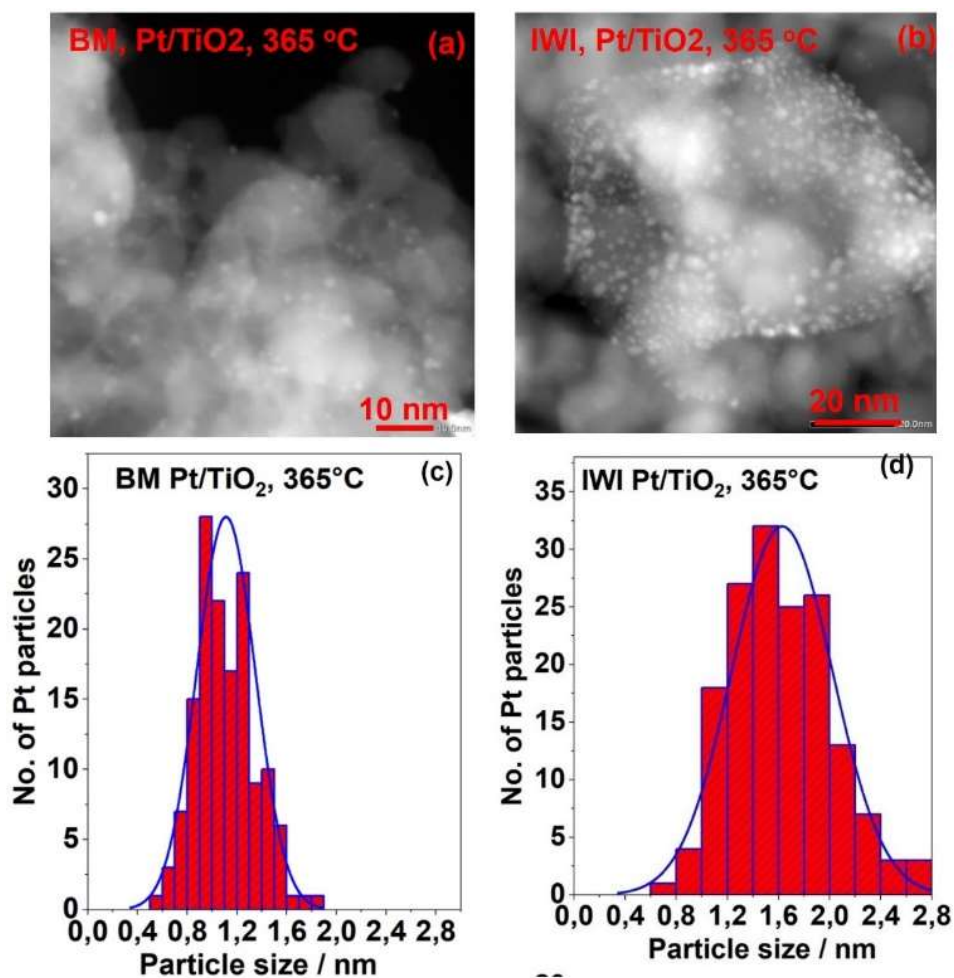


Figure S13. HAADF-STEM images and Pt particle size distributions of the catalysts spent at 365 °C. In panels (a, c) BM Pt/TiO<sub>2</sub> and panels (b, d) IWI Pt/TiO<sub>2</sub>.

### 3.5. XPS

Relative percentage of different Pt species in the fresh and spent catalysts.

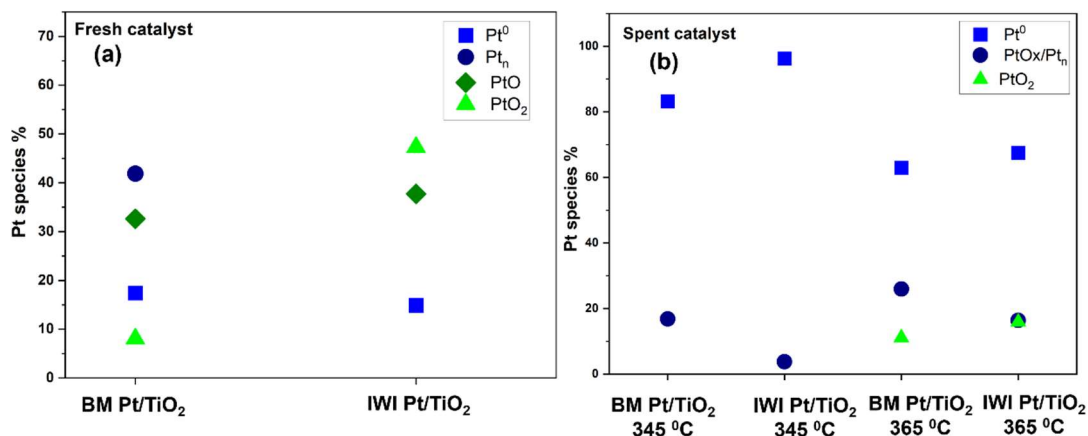


Figure S14. Relative percentage of different Pt species in a) fresh and b) spent catalysts based on the peak intensities observed in the XPS spectra presented in Figures 4 (Fresh catalyst) and 5 (Spent catalyst).

The XPS measured C 1s and Ti 2p spectra of fresh catalysts BM Pt/TiO<sub>2</sub> and IWI Pt/TiO<sub>2</sub> prior to reduction are presented in Figure S15. The C 1s spectrum peak at 285 eV is associated with adventitious carbon, while the 286.3 and 290 eV peaks are linked to carbonate contamination on the catalyst surface. The Ti 2p spectrum peak at 459 eV with a 5.7 eV spin-orbit splitting confirms the presence of TiO<sub>2</sub>. An additional peak at 460 eV observed only of the BM Pt/TiO<sub>2</sub> catalyst could be attributed to TiO<sub>2</sub>-Pt charge transfer due to SMSI.

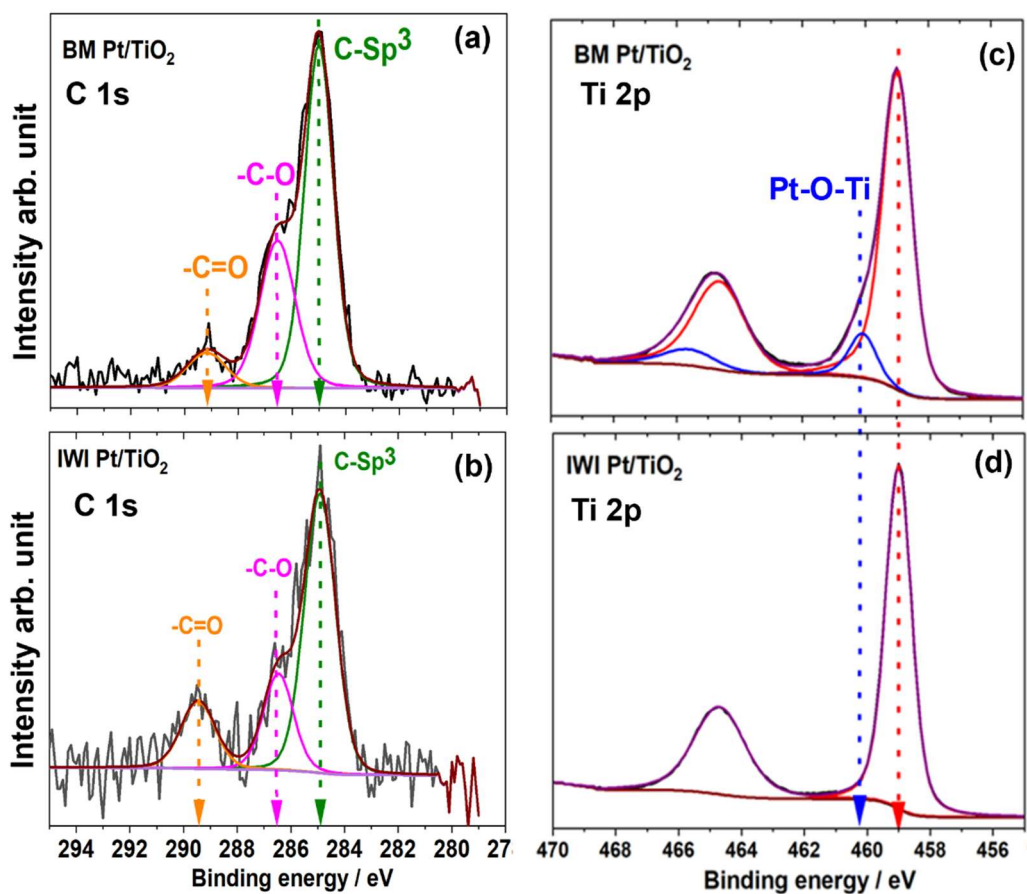


Figure S15. C 1s (a, b) and Ti 2p (c, d) spectra recorded on fresh catalysts.

### 3.6. In situ APXPS

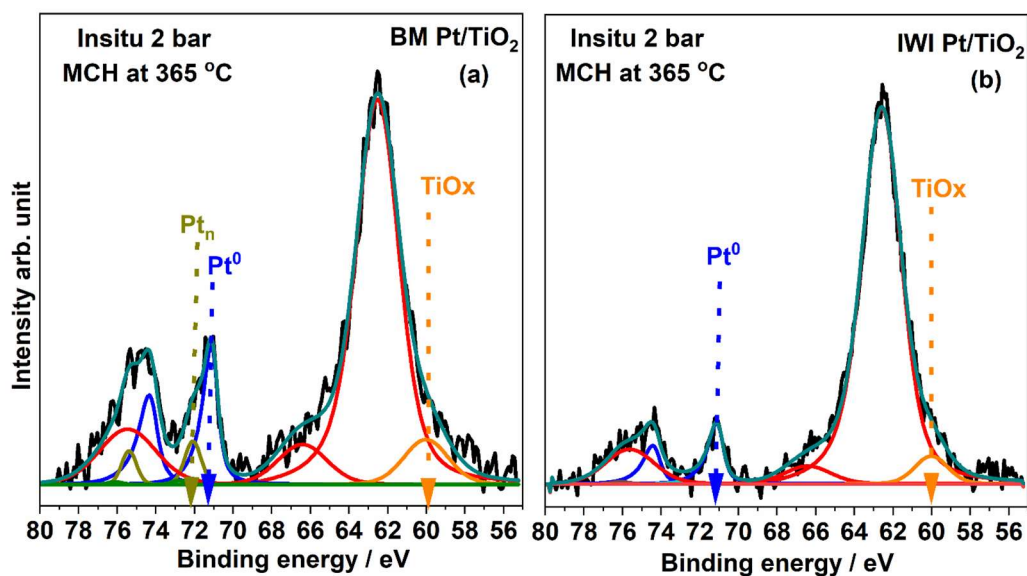


Figure S16. Pt 4f and Ti 3s spectra recorded during the in situ APXPS measurements at 2 mbar MCH pressure and temperatures of 365°C (a) BM Pt/TiO<sub>2</sub> (b) IWI Pt/TiO<sub>2</sub>.

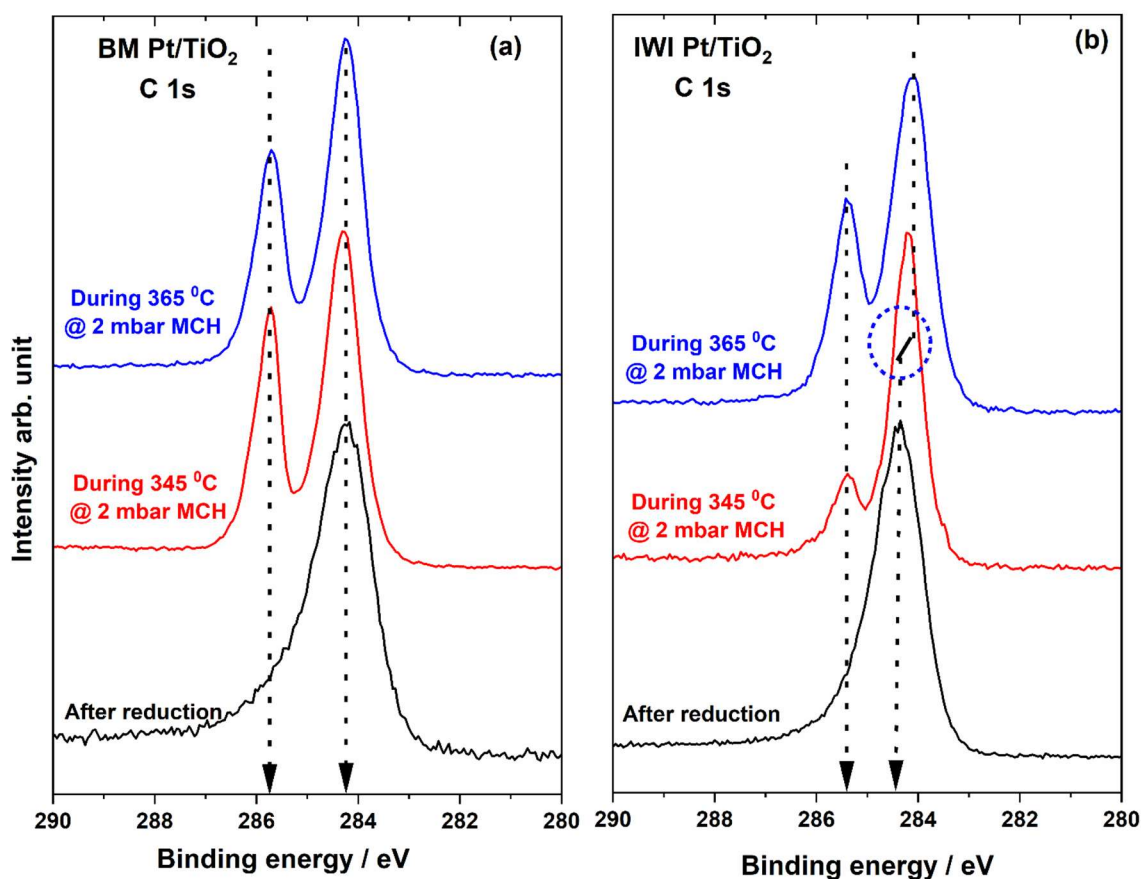


Figure S17. C 1s spectra recorded during the in situ APXPS measurements at 2 mbar MCH pressure and temperatures of 345°C and 365°C for (a) BM Pt/TiO<sub>2</sub> and (b) IWI Pt/TiO<sub>2</sub> catalysts. Highlighted in the image: IWI catalyst 284.4 eV peak shift (0.3 eV) towards lower binding energy under the MCH dehydrogenation conditions.

### 3.7. CO chemisorption

#### *Pretreatment*

Static chemisorption was measured on Micromeritics 3Flex adsorption analyser. 0.4 g of catalyst powder sample was placed in a U-shaped quartz glass tube between quartz glass swabs. Before the CO chemisorption, the catalyst samples were pre-treated as follows. 30 min N<sub>2</sub> flush (50 °C, 50 ml/min), followed by 10 °C/min heating ramp to 110 °C. Gas evacuation to 0.05 mmHg vacuum at 110 °C. H<sub>2</sub> flow (50 ml/min) start at 110 °C and 10 °C/min heating ramp to 350 °C, where the reduction was retained for 1 h, followed by gas evacuation to 0.05 mmHg. The evacuation was continued while the sample was cooled to 35 °C analysis temperature.

#### *Measurement*

In a static chemisorption measurement, first an isotherm of a probe gas adsorption to a sample is measured. Then, the sample is evacuated to a sufficient vacuum to remove physisorbed gas molecules. Last, a second adsorption isotherm is measured, where only physisorption occurs as the chemisorption sites are already occupied. The difference between the first and the second isotherm corresponds to the amount of the chemisorbed probe molecule.

We used CO as our probe molecule, and the adsorption isotherms were measured at 35 °C. Stoichiometry factor of 1.0 was used. CO pressure was varied from 100 to 450 mmHg to obtain the isotherm curves. The sample was evacuated at 35 °C for 1 h to remove physisorbed CO between the two adsorption isotherm measurements. The chemisorption measurement was repeated twice for each sample, and the largest detected difference between the repeated dispersion results was  $\pm 0.5\%$  as absolute units.

### *Isotherms*

The samples analysed were BM Pt/TiO<sub>2</sub> and IWI Pt/TiO<sub>2</sub>. For both samples CO pressure region of 200–450 mmHg produced sufficiently linear isotherms for difference result calculation. The adsorption isotherms and their difference plots are presented in Figure S18.

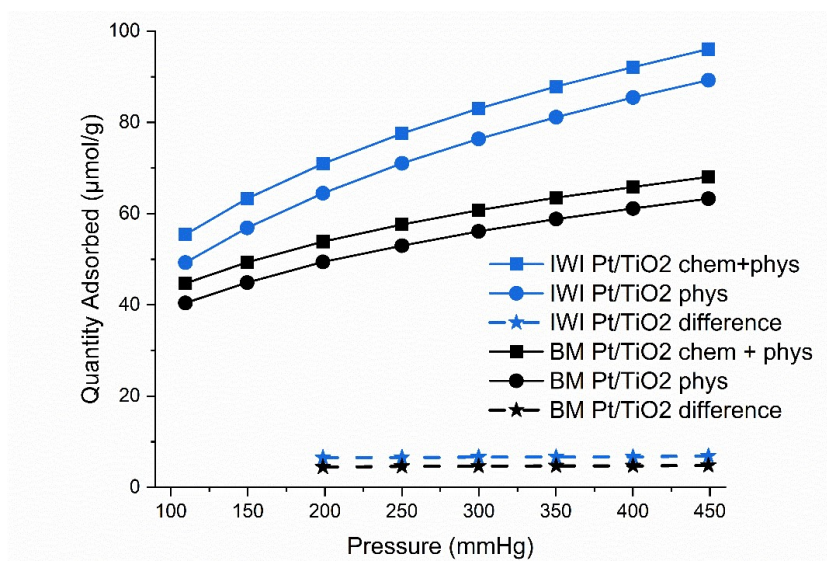


Figure S18. CO adsorption isotherms and isotherm difference plots of BM and IWI Pt/TiO<sub>2</sub>. Chem + phys is the first measured isotherm. Phys is the second measured isotherm.

## 3.8. NH<sub>3</sub> temperature programmed desorption

### *Pretreatment*

NH<sub>3</sub>-TPD was measured on Micromeritics 3Flex adsorption analyser. 0.2 g of fresh catalyst powder sample was placed in a U-shaped quartz glass tube between quartz glass swabs. Before the TPD measurement, the sample was heated to 650 °C at 10 °C/min rate in helium flow (50 ml/min), and the temperature was then retained for 1 h before cooling the sample to 50 °C. NH<sub>3</sub> was adsorbed to the sample for 1 h (5% NH<sub>3</sub> in helium, 50 ml/min) at 50 °C, and excess ammonia was removed by flushing the sample with helium (50 ml/min) for 1 h.

### *Measurement*

The temperature programmed NH<sub>3</sub> desorption heating ramp was 10 °C/min from 50 to 650 °C. Once the highest temperature of 650 °C was reached, it was left to stabilise for 30 min before ending the measurement.

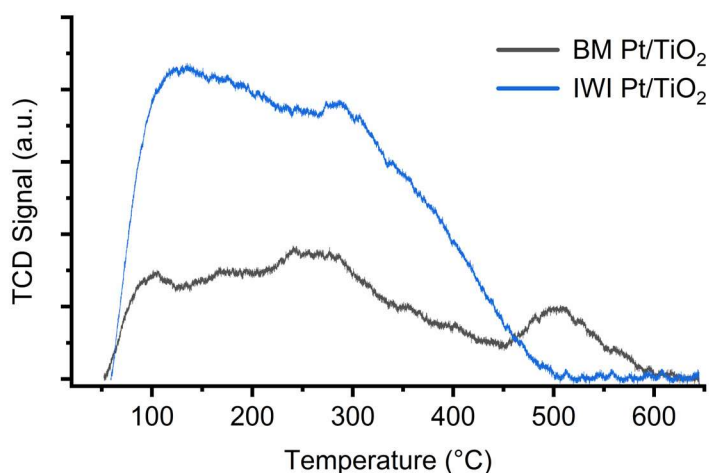


Figure S19. Temperature programmed ammonia desorption plots of BM and IWI Pt/TiO<sub>2</sub>.

### 3.9. Catalyst comparison to literature

Table S3. MCH dehydrogenation hydrogen evolution rates reported in relevant literature. The best available result of each article is reported, i.e. the most active catalyst among the study at its highest conversion during time on stream.

Catalyst	Pt loading wt%	Hydrogen evolution rate mmol H <sub>2</sub> /(g <sub>Pt</sub> *min)	Ref.
BM Pt/TiO <sub>2</sub>	1	670	This article
Pt/CeO <sub>2</sub>	0.15	2509	[7]
Pt <sub>3</sub> (Fe <sub>0.75</sub> Zn <sub>0.25</sub> )/SiO <sub>2</sub>	3	757	[8]
Pt/(TiO <sub>2</sub> + Al <sub>2</sub> O <sub>3</sub> )	0.5	438 <sup>a</sup>	[9]
Pt/La <sub>0.7</sub> Y <sub>0.3</sub> NiO <sub>3</sub>	1	46	[10]
Pt/Al <sub>2</sub> O <sub>3</sub>	1.5	656	[11]
2% Pt 5% Sn/Mg–Al oxide	2	262	[12]

<sup>a</sup> Converted to this unit by us from TOF mol/(mol<sub>Pt</sub>\*h) by assuming that the stated turn over frequency is that of MCH to toluene.

## 4. References

- [1] T. Rude, *et al.*, *Sustainable Energy & Fuels*, 2022, 6, 1541–1553.
- [2] A. Bulgarin, *et al.*, *International Journal of Hydrogen Energy*, 2020, 45, 712–720.
- [3] D.T. Cromer and K. Herrington, *Journal of the American Chemical Society*, 1955, 77, 18, 4708–4709.
- [5] M. Fernandez-Garcia *et al.*, *Chemical reviews*, 2004, 104, 9, 4063–4104.
- [6] M. Fernandez-Garca, *et al.*, *Journal of the American Chemical Society*, 2007, 129, 44, 13604–13612.
- [7] L. Chen, *et al.*, *Nature Communications*, 2022, 13, 1092.

- [8] Y. Nakaya, *et al.*, *ACS Catalysis*, 2020, 10, 5163–5172.
- [9] X. Yang, *et al.*, *Molecular Catalysis*, 2020, 492, 110971.
- [10] A.A. Shukla, *et al.*, *International journal of hydrogen energy*, 2010, 35, 4020–4026.
- [11] C.-X. Chen, *et al.*, *Fuel*, 2024, 360, 130607.
- [12] J. Yan, *et al.*, *International journal of hydrogen energy*, 2018, 43, 9343–9352.